

Experimental observation of spin-exchange-induced dimerization of an atomic one-dimensional system

Nader Zaki,^{1,*} Chris A. Marianetti,¹ Danda P. Acharya,² Percy Zahl,² Peter Sutter,² Junichi Okamoto,¹ Peter D. Johnson,³ Andrew J. Millis,¹ and Richard M. Osgood^{1,†}

¹*Columbia University, New York, New York 10027, USA*

²*Center for Functional Nanomaterials, Brookhaven National Laboratory, Upton, New York 11973, USA*

³*Condensed Matter Physics & Materials Science, Brookhaven National Laboratory, Upton, New York 11973, USA*

(Received 23 August 2012; revised manuscript received 19 October 2012; published 18 April 2013)

Using low-temperature scanning tunneling microscopy, we demonstrate a one-dimensional system that undergoes a charge-density-wave (CDW) instability on a *metallic* substrate. For our measurements we utilize a self-assembled monatomic chain of Co atoms aligned by the steps on a vicinal Cu(111) surface. We assign the measured CDW instability to ferromagnetic interactions along the chain. We show that though the linear arrayed dimers are not electronically isolated, they are magnetically independent, and hence can potentially serve as a binary spin-memory system.

DOI: [10.1103/PhysRevB.87.161406](https://doi.org/10.1103/PhysRevB.87.161406)

PACS number(s): 81.07.Vb, 68.65.-k, 71.27.+a, 72.15.Nj

As has been shown with zero-dimensional (0D) quantum dots and two-dimensional (2D) single-layer atomic sheets, one-dimensional (1D) atomic systems are expected to exhibit novel quantum mechanical phenomena due to angstrom-scale confinement.^{1,2} The realization of true self-assembled monatomic 1D systems which exhibit rich phenomena beyond quantum-well-like behavior,³ however, has been rare.^{4,5} Most attempts have consisted of wire growth on semiconducting surfaces^{6–11} in order to reduce substrate interaction; these experiments have typically observed a charge-density-wave (CDW) instability² commensurate with a metal-to-insulator transition. However, these 1D systems have suffered from an inability to directly determine the crystallographic structure and element constituency of the wires and the modified substrate surface.^{2,11} Furthermore, there remains disagreement on the physical cause of the distortion, whether it be Peierls, Fermi nesting, or phonon interaction.²

Most, if not all, existing reports² of monatomic-wire CDW instabilities involve systems composed of heavy metal elements such as Au and In with completely filled *d* shells and partially filled *s* and *p* orbitals. These limited examples raise a pressing question as to whether density-wave instabilities can occur in other generic material systems, particularly for light elements with partially filled *d* orbitals, and if they can occur on substrates besides semiconducting surfaces.

Here we present low-temperature scanning tunneling microscopy (LT-STM) observations of a dimerization (bond-centered density wave with a wave vector of $k = \frac{\pi}{a}$) instability of a Co atomic-wire system self-assembled on a vicinal Cu(111) substrate. Our earlier studies¹² have shown that these monatomic wires, formed at 300 K, are precisely aligned along the Cu step edges; our STM measurements enable measurement of the chain geometry and atomic positions. Using *ab initio* theoretical calculations we show that the partially filled *d* shells, in fact, drive the instability. Further, in contrast to systems in previous 1D experiments, the instability in Co atomic wires is found to be a consequence of strong local correlations on the 1D-aligned Co atoms. The strong local correlations result in the *d* shell of each Co ion being in a high-spin configuration; the combination of locally maximal spin

and partial orbital filling leads to ferromagnetic correlations, which enhance the dimerization instability.

The experiments reported here are based on our self-assembly-based growth procedure, described elsewhere.^{12,13} This procedure maximizes Co-wire nucleation at the Cu step edges, while minimizing Cu-terrace substitution by Co atoms, as well as any Co island formation; this result is evidenced by the sparse presence of Co atoms in or on the step terrace (Figs. S1–S3). Unlike the case of self-assembled chains on semiconducting substrates,^{2,11} the location of the atomic chains in this bimetallic system is unambiguous; as shown in the Supplemental Material,¹³ we are able to measure the position of the Co atoms precisely due in part to the contrast in density of states of the two metals. We refer the reader to the Supplemental Material¹³ for also an extensive amount of experimental measurements.

An example of our LT-STM measurement of the self-assembled Co chains is shown in Fig. 1(e). This LT-STM instrument is designed for high-resolution microscopy, spectroscopy, and precise atom manipulation and shows very high stability and extremely low drift when operated at 5 K. An instrument of the same type has recently been used for imaging organic molecules by noncontact atomic force microscopy in unprecedented detail.¹⁴ Here, this stability was essential for making the precise lateral atom position measurements that are fully described in the Supplemental Material.¹³ The measurement shows two Cu step edges, visible as a corrugation of the background topography, along which Co atoms (visible as features above the background level) have arranged themselves to form a 1D chain. At 5 K, these chains do not consist of equally spaced Co atoms. A lateral distortion is clearly evident, indicating that the chain is dimerized. The typical measured 1D unit cell width of 5.1 Å matches well with twice the Cu-Cu atom spacing of the ideal Cu(111) substrate (2×2.56 Å).

The measured Co-Co bond length of 2.0(± 0.1) Å (see Supplemental Material,¹³ Fig. S4) is noticeably shorter than the Cu-Cu atom spacing of 2.56 Å, based on our STM measurements over a set of Co chains at 5 K. By comparison, the Co-Co atom distance in self-assembled Co triangle islands

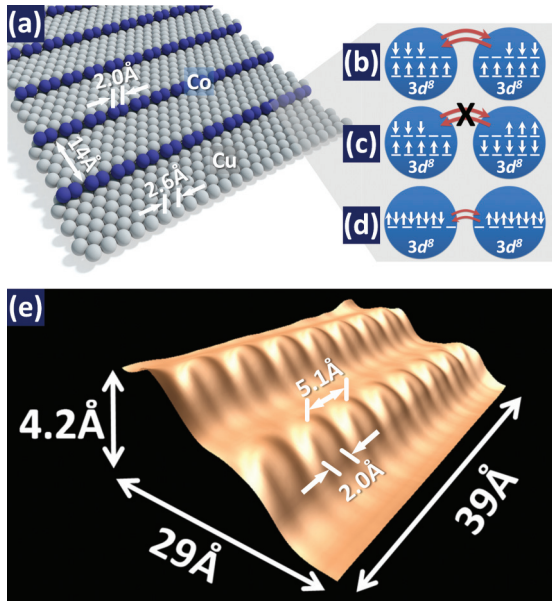


FIG. 1. (Color online) Self-assembled Co atomic chain system. (a) Illustration of dimerized Co atomic chains on vicinal (8.5° miscut) Cu(111). (b)–(d) Illustration of high-spin ferromagnetic, high-spin antiferromagnetic, and zero-spin electron configurations. Coupling is strongest for the high-spin ferromagnetic phase, weaker for the zero-spin phase, and blocked for the antiferromagnetic phase. (e) Perspective view of a STM topography of two self-assembled Co wires at adjacent Cu step edges. The vertical scale has been magnified to accentuate the appearance of the Co wires. The Co atoms constituting these wires have undergone a 1D structural distortion, leading to the appearance of a single peak near the Cu step edge. However, the underlying Co atoms constituting each single peak are resolved farther away from the Cu step edge due to the decreased contribution of the Cu local density of states to the tunneling current. Constant current tunneling parameters: $V_{\text{bias}} = +0.742$ V at 9.4 nA.

on Cu(111) ranges from 2.50 to 2.56 Å,¹⁵ which is comparable to that found in bulk Co. It is surprising that the Co chain would exhibit a structural distortion; given that the atom spacing of bulk Co is similar to bulk Cu (a difference of only $\sim 2\%$), an ideal uniform Co atom spacing would be expected. It therefore appears that the bond-length distortion in this case is due to the one-dimensional geometry along the Cu step edge with its anisotropic environment. Our observation of a dimerized Co chain is also unexpected since monatomic Cu chains on Cu(111), which are fabricated using atom-tip manipulation, do not exhibit such a distortion;¹⁶ these experimental results used STM measurements at 7 K. Hence, the fact that we are using Co rather than Cu is important for the onset of this distortion.

One expects that the lattice distortion is a low-temperature phenomenon, occurring only below a critical temperature, as observed for wires on semiconducting surfaces. The bimetallic Co/Cu(775) system investigated here undergoes a phase transition at relatively elevated temperatures. At a temperature of 91 K, the Co distortion is nonuniform along a chain, varying from 0.6 to 0.0 Å. The Co chains also show a tip-bias dependency; at low tip bias, single Co atoms are easily resolved, while at higher tip bias, a $\times 2$ periodicity is more

prevalent (Figs. S9 and S10). At a slightly lower temperature of $81 (\pm 4)$ K, however, some chains appear exactly as those measured at 5 K, i.e., they possess a dimerization instability that is independent of tip bias (Fig. S11). These observations indicate a coexistence of two different phases, leading to the tentative assignment of this system change as a first-order phase transition with a critical temperature in the vicinity of 100 K.

To understand the physics of the dimerization as observed in our experimental measurements, we examine theoretically how and why an isolated Co chain restricted to distortions in one spatial dimension dimerizes. The effect of the step may be subsequently deduced. *Ab initio* and density functional theory (DFT) calculations have previously been performed for free¹⁷ and surface supported finite¹⁸ and infinite atomic chains¹⁹ with results ranging from nondimerized to zigzag to anisotropically strained. However, no clear physical mechanism has been deduced or put forward. Here we present DFT calculations, based on several different functionals (Figs. S5 and S6),¹³ which shed light on the physics underlying our experimental observations. Specifically, the energy of an infinite length 1D periodic system consisting of two Co atoms per unit cell was studied under the constraint that the period of the system matched twice the Cu atom-atom spacing (2×2.56 Å) and that the Co atoms are allowed to move only along the wire direction. With regard to the latter constraint, note that our earlier *experimental* observations have shown the chain is in fact linear. In addition, our calculations used energy minimization to identify the final atom configuration. Finally, notice that in our experiment, the vicinal Cu(111) substrate template serves to align the atoms in the chain in a *linear* 1D array.

In our theoretical model there are two Co-Co bond lengths. Figure 2(a) shows the dependence of the energy on the length of the shorter, i.e., nearest-neighbor, Co-Co bond (measured relative to the mean Co-Co distance). A clear energy minimum is visible at $d_{\text{short}} = 0.794d_{\text{avg}} = 2.03$ Å (implying $d_{\text{long}} = 3.08$ Å). A key result of the DFT calculation is that the Co *d* shell on each site is essentially fully spin polarized, having maximal spin polarization for a given *d* occupancy. Different orientations of the Co spin were investigated [Fig. 2(a) shows as an example the energy of the two sublattice antiferromagnet]; the ground state was found to be in the *ferromagnetic* phase. Furthermore, the ferromagnetic phase favors a structural distortion while the antiferromagnetic phase does not. These findings suggest that the dimerization instability is driven by the energetics of electron transfer between *d* orbitals subject to a ground state of maximal spin. Because the *d* orbitals are partially occupied, transfer is optimized in a ferromagnetic state, while the high-spin state means that electron transfer is essentially forbidden in the antiferromagnetic state. These considerations suggest that the spin-polarized *d* orbitals play a key role in the dimerization phenomenon and thus spin (magnetic) interactions are key to our observations.

To further investigate the relevance of the *d* orbitals to the dimerization we compare in Fig. 2(b) the dimerization energetics of stretched wires of Co (partially filled *d* shell; DFT predicts a ferromagnetic ground state) and Cu (fully filled *d* shell; DFT predicts a paramagnetic ground state) wires. In general grounds, we expect that a physical 1D system that is stretched to have a mean bond length sufficiently far from its

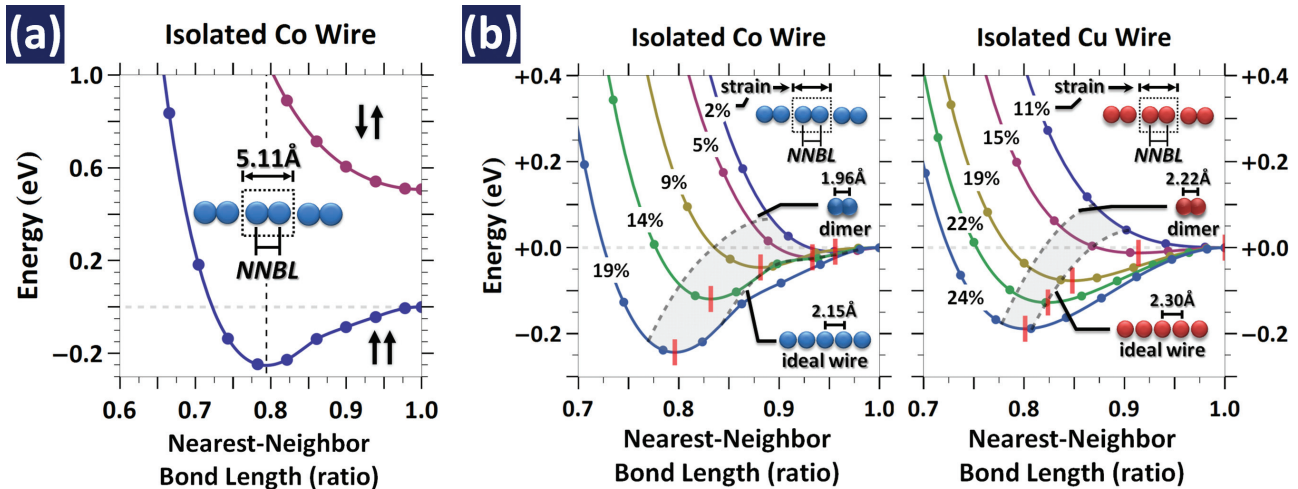


FIG. 2. (Color online) DFT energy-phase diagrams for atomic wires. Points denote actual calculated energies while smooth lines in between are third-order interpolations. Total energies were calculated for a two-atom unit cell using DFT and the GGA functional (Figs. S5 and S6). The lack of smoothness in some regions is due to varying degrees of orbital polarization [see Supplemental Material (Ref. 13)]. (a) Energy-phase diagram for Co atomic wire. The energies of the Co wires have been offset with respect to the *ferromagnetic* nondistorted case (NNBL = 1.0); the horizontal dashed gray line denotes the reference. The nearest-neighbor bond length is given as a ratio of the bulk Cu atom spacing (2.5561 Å). (b) Energy of Co_2 and Cu_2 isolated wires measured relative to the energy of the undimerized wire and plotted against degree of dimerization (parametrized as the ratio of the short bond length to the average bond length). Different curves indicate different strains (i.e., different unit cell lengths) relative to the unit cell length that minimizes the DFT energy of the wire. The energy of the Co wire has been computed for a ferromagnetic state; the Cu wire was computed for a non-spin-polarized state (spin-polarized calculations converged to a zero-spin state). The left hand dashed gray line denotes the optimal bond length of the dimer (measured in units of one half of the mean unit cell length of the strained wires). The right hand gray line indicates the interatomic distance for the optimal nondistorted wire. The red vertical line segments mark the optimal nearest-neighbor bond length for each respective strained wire system.

ideal bond-length spacing will undergo a distortion. However, both the extent of the strain required for dimerization and the amplitude of the distortion will depend on the physics responsible for the instability. In the two panels of Fig. 2(b) we plot the energy (relative the energy of the undimerized state) versus the degree of dimerization, for different amounts of strain relative to the bond length which minimizes the DFT energy for the undimerized wire. We see that in the Co system the dimerization becomes favored at a much lower strain than in the Cu system, and the energy gain from dimerization is much greater for equal amounts of strain. We also compare the optimal length of the short bond (indicated by the red vertical line) to the optimal spacing of the transition metal dimer (leftmost gray dashed line) and to the optimal atom-atom distance in the unstrained wire (rightmost gray dashed line). For a strained Co wire, the nearest-neighbor bond length generally lies between the optimal dimer bond length and the optimal nondistorted wire bond length, indicating that dimerization is truly favored. By contrast, in the case of a strained Cu wire, the nearest-neighbor bond length is generally greater than, but close to, the optimal nondistorted wire bond length (at least for strains up to $\sim 22\%$).

This comparison of Co and Cu atom wires highlights the difference in tendency to dimerization in a partially filled d -orbital derived band 1D system versus a partially filled sp -orbital derived band 1D system. To further probe the physics of the dimerization, we note that the absence of the dimerization in the antiferromagnetic state indicates that the dimerization is connected to hopping of d electrons (suppressed in the antiferromagnetic state by the condition

that each Co ion is in a high-spin configuration). The total d occupancy is approximately d^8 . Choosing an angular-momentum quantization axis (z direction) parallel to the chain direction we note that the $3d_{xy}$ and $3d_{x^2-y^2}$ orbitals do not hybridize much along the chain and instead act as local moments (Fig. S7). The physics is driven by the $3d_{xz}$, $3d_{yz}$, and $3d_{z^2}$ orbitals. In the spin-polarized state, the majority orbitals are filled while the minority orbitals are nearly half filled. In this circumstance, a dimerization instability leads to a large energy gain, which arises because in each orbital there is one minority spin electron per pair of atoms; this electron forms a strong bond in the dimerized state, with the antibonding orbital completely empty. This result can be viewed as a Peierls distortion. Note that if the ground state was not high spin, the band energetics would be less favorable to dimerization because one would have partially, not fully, occupied bonds. The dimerization instability is also favored by the relatively localized nature of the d electrons which, in contrast to the more spatially extended s - p electrons, have predominately a nearest-neighbor hopping, and which moreover rises rapidly as the interatom distance is decreased.

The above physical explanation is only reasonable if the hybridization of the Co d states to the electrons in the vicinal Cu substrate is relatively weak. This hypothesis is consistent with the observation of weak indirect spin exchange interaction for Co dimers on Au(111) and Cu(100) substrates.^{20,21} These studies found that although there exists a strong indirect exchange for a Co monomer by way of the Kondo effect (indicating the presence of a moment, i.e., a locally high-spin configuration, on the Co site), a Kondo signal was lacking for a

Co dimer that was fabricated by STM atom-tip manipulation. The lack of a Kondo signal for the dimer is naturally understood in terms of the non-negligible d - d electron transfer suggested here. Note, however, that the substrate is important in our 1D system, in that, as mentioned above, it provides strain and linearly aligns the Co atoms; both of these effects are seen in our STM data.

In order to further elucidate the substrate/Co chain interactions, we have also performed local density approximation (LDA) and generalized gradient approximation (GGA) calculations for a Co chain *on a Cu step*. We find that, within DFT, bonding of the chain to the stepped substrate eliminates the dimerization. Note that our DFT procedure was first tested on a standard Cu(111) substrate and found to yield the expected Cu electronic structure. We attribute the lack of Co dimerization to the fact that DFT is unable to accurately capture the detailed physics. It is likely that this failure occurs because DFT overestimates the hybridization between the chain and the substrate; we are currently working to understand the DFT failure more clearly. We note that our result does not affect the mechanism we introduce to understand the dimerization, which, as discussed above, is consistent with other spin-substrate interactions.

One important feature of our experimental chains is best seen in the spin behavior within our chains; thus we first examine the spin properties and then explore the consequences of this behavior for a magnetic memory. An important consequence of the bond-length distortion is a strongly decreased electron transfer between neighboring 2-Co-atom unit cells, implying also that the coupling of spin between dimers becomes negligible. In order to quantify this, we perform a cluster expansion of the total energy in terms of the spin cluster functions. Given a lattice model with a binary-site variable (i.e., up or down spin), one can perform a power-series expansion of any average lattice observable in terms of the correlation functions of the site variables. In spin systems, one can often obtain a highly accurate expansion using only pair terms over a short range. We find that one can accurately represent the energetics using only neighbor-pair terms, as defined in the following equation:

$$H = E_0 + \sum_i J_1 s_i \cdot s_{i+1} + J_2 s_{i+1} \cdot s_{i+2},$$

where E_0 is the nonmagnetic energy contribution, s is ± 1 , and J_1/J_2 are the neighbor magnetic pair interactions [Fig. 3(a) and Fig. S8(a)].¹³ The goal of using this basic model is to show the change in these parameters as a function of distortion. In Fig. 3(b), a plot of the parameters is shown (Fig. S8). Note that in the undistorted wire the magnetic interaction constants are equal by symmetry, with the negative sign arising because DFT favors a ferromagnetic state. As the system is distorted, J_1 increases rapidly in magnitude whereas J_2 goes quickly to zero. We also present the sum of the magnetic-interaction parameters ($J_1 + J_2$), which gives the total magnetic contribution to the energy. The monotonic decrease of the sum ($J_1 + J_2$) as distortion is increased also shows that the ferromagnetic state strongly favors the distortion, as expected if the driving force is electron transfer between high-spin configuration d states. Note that, except for an insignificant decrease near the non-dimerized bond

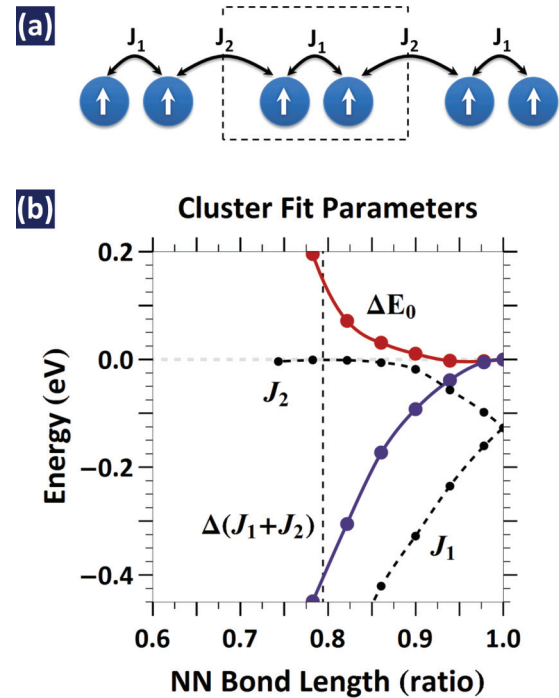


FIG. 3. (Color online) Fitting to a cluster expansion model. (a) Cluster expansion model illustration of the Co 2-atom unit cell. J_1 denotes the nearest-neighbor or *intrapair* interaction while J_2 denotes the *interpair* interaction. The unit cell is delineated by the dashed rectangle outline. (b) Cluster expansion model parameter fits for the Co atom wire for different amounts of distortion. E_0 is the nonmagnetic energy contribution. The vertical dashed line denotes the optimal Co wire distortion. Note that J_2 is quite negligible at the optimal distortion length. Energies were computed using spin-polarized GGA (Fig. S8).

length, E_0 is monotonically increasing; this illustrates that nonmagnetic terms do not play a role in the dimerization.

The striking difference in the variation of the magnetic-interaction parameters, J_1 and J_2 , under dimerization suggests that the spin chain may provide an interesting realization of a memory device. In the dimerized state, J_2 is negligible compared to the quite large magnetic coupling, J_1 , between nearest neighbors. A consequence of this result is that while each dimer is itself in a high-spin state, the spins of neighboring dimers may take arbitrary orientations with negligible energy penalty. Hence, a dimerized Co spin chain can potentially behave as a linear array of spin-memory bits. Binary memory requires a bistability, in other words, an easy axis for the magnetization of a dimer. We expect that this is provided by the Cu step edge, as was shown for a Co/Pt(997) system.²² A somewhat similar system, but based on antiferromagnetic switching, has been recently realized using Fe on Cu₂N.²³ Finally, we note that even though the Co chain unit cells may be “spin isolated,” they are not electronically disjoint; an energy band diagram of the Co chain reveals band crossings (predominately of d_{z^2} and s character) at the Fermi energy (Fig. S7), suggesting a possibility for manipulating the spin states via appropriately applied currents.²⁴

Our experimental results and the CDW phenomena seen here also have implications to the field of suspended atomic

chains formed by break junctions.²⁵ While it has been found that suspended nonmagnetic wires can be formed by this method, forming suspended magnetic wires has not yet been successful.²⁶ The reasoning for this was reported to be softening of the binding energy of the atomic chain due to magnetism.²⁶ While the process of forming a suspended chain is complicated,²⁷ the results reported here suggest that forming a suspended Co atomic chain is difficult, in part, due to the tendency for the chain to dimerize. The long bond would be weakened due to the extent of the dimerization occurring during stretching of the chain [Fig. 2(b)].

Thus both our experimental and theoretical results show a Co atomic wire on stepped Cu(111) behaves as a 1D atomic system with a low-temperature spin-exchange-induced

dimerization instability. This work raises the question as to whether other light partially filled *d*-orbital 1D systems will exhibit a similar instability once realized in experiment, and their possible technological applications.

This work was supported by the Department of Energy, Office of Basic Energy Sciences, Division of Materials Sciences and Engineering under Award Contract No. DE-FG 02-04-ER-46157. Work at Brookhaven National Laboratory was supported by the Department of Energy under Contract No. DE-AC02-98CH10886. We thank Mark Hybertsen for discussions and suggestions regarding the DFT calculations. We thank James Davenport and Abhay Pasupathy for helpful discussions.

*Corresponding author: nz2137@columbia.edu

†Corresponding author: osgood@columbia.edu

¹V. V. Deshpande, M. Bockrath, L. I. Glazman, and A. Yacoby, *Nature (London)* **464**, 209 (2010).

²P. C. Snijders and H. H. Weitering, *Rev. Mod. Phys.* **82**, 307 (2010).

³N. Nilius, T. M. Wallis, and W. Ho, *Science* **297**, 1853 (2002).

⁴H. Weitering, *Nat. Phys.* **7**, 744 (2011).

⁵C. Blumenstein, J. Schäfer, S. Mietke, S. Meyer, A. Dollinger, M. Lochner, X. Y. Cui, L. Patthey, R. Matzdorf, and R. Claessen, *Nat. Phys.* **7**, 776 (2011).

⁶O. Gurlu, O. A. O. Adam, H. J. W. Zandvliet, and B. Poelsema, *Appl. Phys. Lett.* **83**, 4610 (2003).

⁷J. Wang, M. Li, and E. I. Altman, *Phys. Rev. B* **70**, 233312 (2004).

⁸J. N. Crain, A. Kirakosian, K. N. Altmann, C. Bromberger, S. C. Erwin, J. L. McChesney, J.-L. Lin, and F. J. Himpsel, *Phys. Rev. Lett.* **90**, 176805 (2003).

⁹J. R. Ahn, J. H. Byun, H. Koh, E. Rotenberg, S. D. Kevan, and H. W. Yeom, *Phys. Rev. Lett.* **93**, 106401 (2004).

¹⁰K. R. Simov, C. A. Nolph, and P. Reinke, *J. Phys. Chem. C* **116**, 1670 (2012).

¹¹H. J. W. Zandvliet, A. Houselt, and B. Poelsema, *J. Phys.: Condens. Matter* **21**, 474207 (2009).

¹²N. Zaki, D. Potapenko, P. D. Johnson, and R. M. Osgood, *Phys. Rev. B* **80**, 155419 (2009).

¹³See Supplemental Material at <http://link.aps.org/supplemental/10.1103/PhysRevB.87.161406> for methods, additional discussion and figures.

¹⁴L. Gross, F. Mohn, N. Moll, P. Liljeroth, and G. Meyer, *Science* **325**, 1110 (2009).

¹⁵M. V. Rastei, B. Heinrich, L. Limot, P. A. Ignatiev, V. S. Stepanyuk, P. Bruno, and J. P. Bucher, *Phys. Rev. Lett.* **99**, 246102 (2007).

¹⁶S. Fölsch, P. Hyldgaard, R. Koch, and K. H. Ploog, *Phys. Rev. Lett.* **92**, 056803 (2004).

¹⁷C. Ataca, S. Cahangirov, E. Durgun, Y.-R. Jang, and S. Ciraci, *Phys. Rev. B* **77**, 214413 (2008).

¹⁸Š. Pick, P. A. Ignatiev, A. L. Klavskyuk, W. Hergert, V. S. Stepanyuk, and P. Bruno, *J. Phys.: Condens. Matter* **19**, 446001 (2007).

¹⁹Y. Mokrousov, G. Bihlmayer, S. Blügel, and S. Heinze, *Phys. Rev. B* **75**, 104413 (2007).

²⁰W. Chen, T. Jamneala, V. Madhavan, and M. F. Crommie, *Phys. Rev. B* **60**, R8529 (1999).

²¹P. Wahl, P. Simon, L. Diekhöner, V. S. Stepanyuk, P. Bruno, M. A. Schneider, and K. Kern, *Phys. Rev. Lett.* **98**, 056601 (2007).

²²P. Gambardella, A. Dallmeyer, K. Maiti, M. C. Malagoli, W. Eberhardt, K. Kern, and C. Carbone, *Nature (London)* **416**, 301 (2002).

²³S. Loth, S. Baumann, C. P. Lutz, D. M. Eigler, and A. J. Heinrich, *Science* **335**, 196 (2012).

²⁴G. D. Mahan, *Phys. Rev. Lett.* **102**, 016801 (2009).

²⁵A. I. Yanson, G. R. Bollinger, H. E. van den Brom, N. Agrait, and J. M. van Ruitenbeek, *Nature (London)* **395**, 783 (1998).

²⁶A. Thiess, Y. Mokrousov, S. Heinze, and S. Blügel, *Phys. Rev. Lett.* **103**, 217201 (2009).

²⁷F. Tavazza, D. T. Smith, L. E. Levine, J. R. Pratt, and A. M. Chaka, *Phys. Rev. Lett.* **107**, 126802 (2011).